JOURNAL OF GEOPHYSICAL RESEARCH, VOL. 102, NO. A4, PAGES 7331-7343, APRIL 1, 1997

Investigations of thermospheric-ionospheric dynamics with 6300-Å images from the Arecibo Observatory

Michael Mendillo, Jeffrey Baumgardner, Daniel Nottingham, and Jules Aarons

Center for Space Physics, Boston University, Boston, Massachusetts

Bodo Reinisch and James Scali

Center for Atmospheric Research, University of Massachusetts, Lowell

Michael Kelley

School of Electrical Engineering, Cornell University, Ithaca, New York

Abstract. Pilot observations were conducted at Arecibo, Puerto Rico, using an all-sky, image-intensified CCD camera system in conjunction with radar, ionosonde, and Global Positioning System (GPS) diagnostic systems during the periods January 19-28, 1993, and February 21 to August 22, 1995. These represent the first use of campaign mode operations of an imager at Arecibo for extended periods of *F* region observations. The January 1993 period (the so-called "10-day run") yielded a rich data set of gravity wave signatures, perhaps the first case of direct imaging of thermospheric wave train properties in the *F* region. The 6-month 1995 campaign revealed two additional optical signatures of *F* region dynamics. A brightness wave in 6300 Å passing rapidly through the field of view (FOV) has been linked to meridional winds driven by the midnight temperature maximum (MTM) pressure bulge. On May 3, 1995, during a period of geomagnetic activity, a 6300-Å airglow depletion pattern entered the Arecibo FOV. Such effects represent the optical signatures of equatorial spread *F* instabilities that rise above the equator to heights near 2500 km, thereby affecting Arecibo's $L = 1.4$ flux tube.

1. Introduction

The incoherent scatter radar (ISR) at the Arecibo Observatory (18.3°N, 66.75°W) has a rich history of contributions to upper atmospheric science [*Gordon*, 1964; *Kelley*, 1989]. Recent upgrades to the Arecibo radar [*Campbell*, 1995] and its colocated optical facilities [*Tepley*, 1995] will result in an enhanced capability for multidiscipline research over an altitude range from the troposphere to the plasmasphere. In this paper, we report on pilot observations using an all-sky airglow imaging system. While such instruments operate on a routine basis with ISR facilities in Sondrestrom (Greenland), Millstone Hill (Massachusetts), and Jicamarca (Peru), results reported on here represent the first use of all-sky imaging as a patrol diagnostic capability at Arecibo.

2. Background

The Arecibo site is usually considered to be a "pure midlatitude" site in that its upper atmosphere is not routinely influenced by the penetration of auroral processes to midlatitudes, as occurs at Millstone Hill [*Providakes et al.*, 1989; *Buonsanto et al.*, 1992; *Foster et al.*, 1994]. While its geographic latitude (≈18°) results in solar input that might describe its thermosphere as low latitude or tropical, as done for geophysical observations in Arequipa, Peru (16.4°S), Maui (20.8° N), Cachoeira Paulista, Brazil (22.7°S), and Manila (14°N), the tilt of the Earth's dipole axis results in a relatively high magnetic latitude (~30°) and, consequently, a high magnetic inclination angle ($I \approx 50°$). This causes thermospheric dynamics to have dramatic ionospheric consequences since induced vertical motions are most effective where the geometrical coupling factor $\sin I \cos I$ reaches its maximum value (at $I = 45°$) [*Rishbeth and Garriott*, 1969; *Kelley*, 1989].

Processes associated with equatorial and low-latitude aeronomy are generally considered to be important where $I \leq 35°$, that is, at magnetic latitudes bound by the regions of the Appleton anomaly in *F* region electron densities and their associated intertropical airglow arcs (dip latitude with $\phi \leq \pm 20°$). For a dipole field these are related by $\tan I = 2\tan\phi$; the geomagnetic field line spanning this region reaches ~1000 km above the geomagnetic equator ($L \approx 1.16$). Thus the low-latitude ionosphere is usually considered to be defined by the plasma within flux tubes that reach to equatorial apex heights ≤1000 km [*Hanson and Moffett*, 1966], well equatorward of the Arecibo *L* value (≈1.4) that extends to a height of ≈2500 km above the geomagnetic equator.

Because of its geophysical location, as described above, Arecibo is not a site where F-region optical structures are expected on a routine basis. Diffuse aurora, stable auroral red

Paper number 96JA02786.
0148-0227/97/96JA-02786$09.00

(SAR) arcs, and *F* region trough related gradients, common subauroral features seen at Millstone Hill [*Mendillo et al.*, 1989], would appear near Arecibo under only highly active geomagnetic periods. Similarly, *F* region airglow depletions associated with equatorial spread *F* (ESF), as described by *Weber et al.* [1978] and *Mendillo and Baumgardner* [1982], and latitudinal gradients related to variations in position of the intertropical arcs [*Mendillo et al.*, 1992] are not usually considered midlatitude effects. This is not to imply that optical signatures of ionosphere-thermosphere origin do not occur at Arecibo nor that they are time invariant. Indeed, photometry at Arecibo has a long and productive history, ranging from airglow variations produced by the so-called "midnight collapse" of the *F* region [*Nelson and Cogger*, 1971; *Sobral et al.*, 1978] to detection of airglow signatures produced by photoelectrons from conjugate point sunrise [*Carlson*, 1968]. Fabry-Perot interferometry (FPI) has contributed to measurements of the temperature [*Cogger et al.*, 1970] and dynamics [*Burnside et al.*, 1981] of the thermosphere, as well as to pioneering studies of the exosphere [*Meriwether et al.*, 1980; *Kerr and Tepley*, 1988]. Lidars [*Tepley et al.*, 1991, *Kane et al.*, 1993; *Friedman et al.*, 1993] have clearly demonstrated that Arecibo can be an interesting site for optical studies of mesospheric layers and waves. Yet, wide-angle, two-dimensional imaging has not been a routine capability at Arecibo. It has been used for specialized campaigns to observe mesopheric waves (e.g., *Hecht et al.* [1994] during the Arecibo Initiative in Dynamics of the Atmosphere (AIDA) and in Collaborative Observations Regarding the Nightglow (CORN) Campaigns, and by *Taylor and Garcia* [1995] during the January 93 period reported on here); imaging systems have also been used during active experiments involving chemical releases [e.g., *Bernhardt et al.*, 1988b] or RF heating studies [e.g., *Bernhardt et al.*, 1988a].

To explore the upper atmospheric science yield possible for 6300-Å all-sky imaging observations at Arecibo, an all-sky imaging system developed for the National Science Foundation (NSF) Coupling, Energetics and Dynamics of Atmospheric Regions (CEDAR) program was deployed in Puerto Rico as part of the Mafongo Campaign (the so-called "10-day run") from January 19 to 28, 1993. Encouraged by the results obtained in this brief campaign, a subsequent period of extended observations was conducted from February 21 to August 22, 1995. Here we report on the preliminary results to emerge from these pilot studies.

3. Observations of Structures in *F* Region Airglow

The Boston University all-sky-imaging system has been described in detail by *Baumgardner et al.* [1993]. Briefly, it is an image-intensified CCD instrument that uses narrow band filters to observe specific emissions over an all-sky (180°) field of view (FOV). Figure 1 shows the extent of the FOV for ± 75° zenith angle (150° FOV) observations for an assumed mean emission height of 300 km appropriate, under most conditions, for 6300-Å airglow from *F* region recombination chemistry. One goal of the Mafongo campaign was to search for *F* region gravity wave signatures that might be linked to episodes of midlatitude spread *F* [*Fukao et al.*, 1991, *Kelley and Fukao*, 1991]. As a consequence, the imager was operated using only two filters, 6300 Å (on band) and 6444 Å (off-band), in order to get frequent observations calibrated in Rayleighs (R) over the course of each night. *F* region gravity waves have been detected

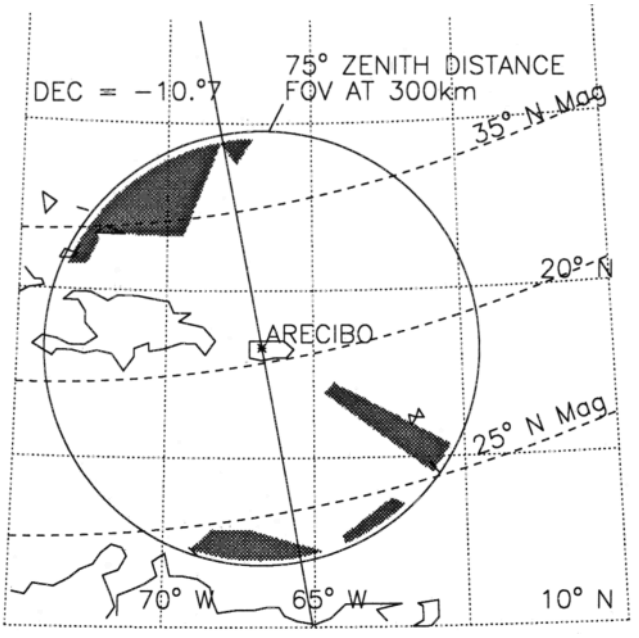

Figure 1. The field of view (FOV) of a 150° "all-sky imager" for an assumed 6300-Å mean emission height of 300 km. The orientation of the geomagnetic meridian in the FOV is given (declination angle ≈ 11°W). Structures associated with the Arecibo Observatory and on the horizons to the northwest and south prevent a full 150° (or 180°) FOV. These regions of no data are omitted from all January 1993 images shown in the figures that follow. For the 1995 observations a different set up was used to lessen this problem (see Figure 7).

for decades using various radio diagnostics to sense their presence as traveling ionospheric disturbances (TIDs). Similarly, periodic variations in photometer and FPI signatures have long been attributed to variations in airglow chemistry associated with gravity wave motions [*Roach*, 1961; *Hines*, 1964]. We believe the "10-day run" campaign to be the first dedicated attempt to obtain two-dimensional images of gravity waves by the 6300-Å airglow structures they induce while propagating at ionospheric *F* region heights.

Figure 2 summarizes the 10-night period of observational seeing conditions, as well as the frequency of wave-like (W) structures encountered. Somewhat to our surprise, wave-like structures were the dominant pattern of activity on clear nights. This is in marked contrast to experience at Millstone Hill where over 900 nights of observations recently characterized (M. Mendillo et al., The CEDAR imager at Millstone Hill: Airglow, stable auroral red (SAR) arcs, and the diffuse aurora, manuscript in preparation, 1997) do not include even a category for 6300-Å wave-like structures. It may be that at a subauroral site, such structures as diffuse aurora, SAR arcs and the trough so dominate the all sky pattern that weak gravity wave signatures are not recognized; nevertheless, even on nights of uniform airglow, no wave-like signatures are readily apparent in 6300-Å images at Millstone Hill. They are, however, occasionally seen in mesosphere regions using 5577-Å observations. The high dip angle ($I \cong 72°$) at Millstone Hill, as mentioned above, is also not as favorable for wind-induced vertical motions of plasma into and out of the 6300-Å airglow generation layers as it is at Arecibo.

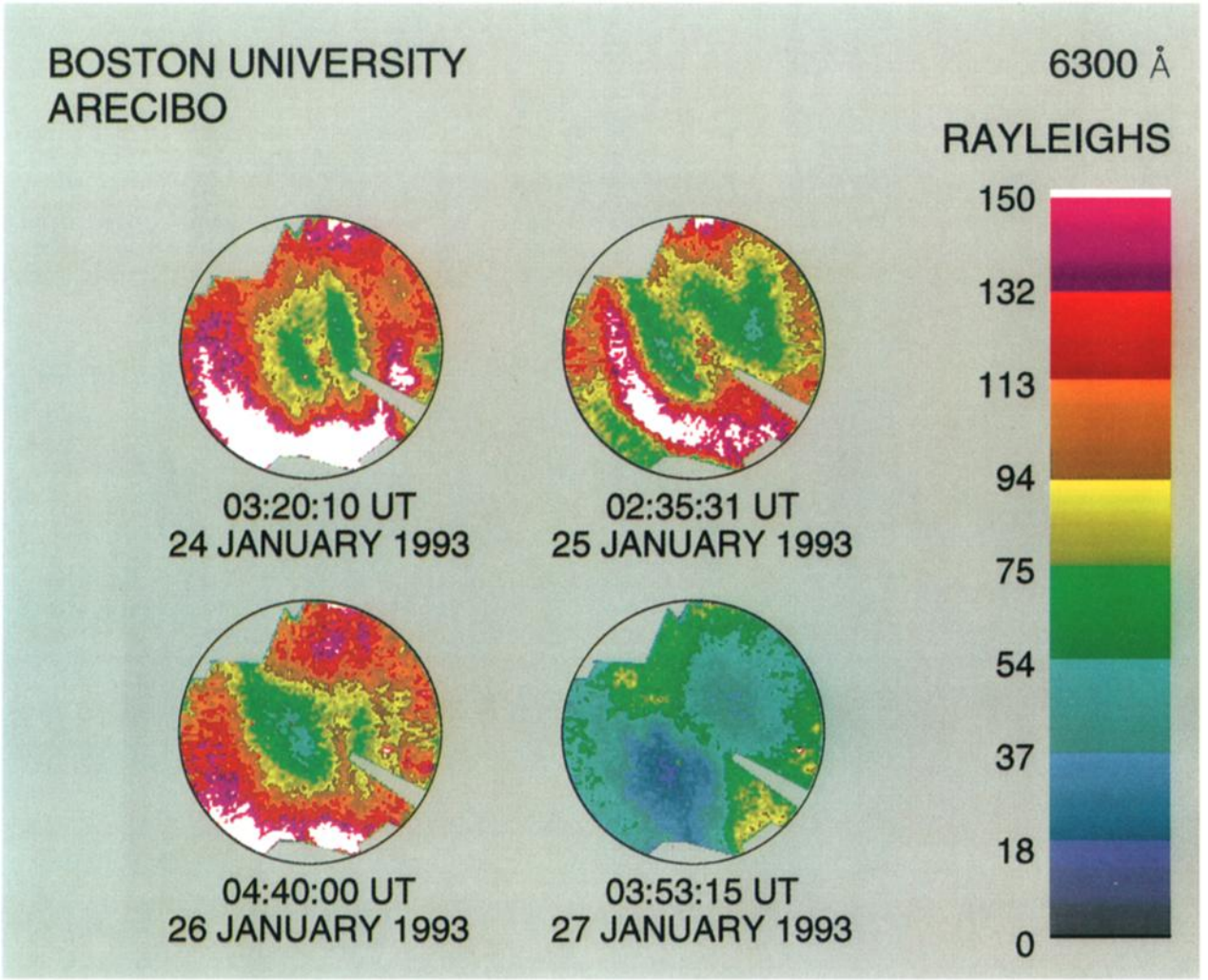

Plate 1. Examples of 6300-Å airglow structure present in all-sky imaging observations on four consecutive nights in January 1993. Note that the patterns of enhancement and depletion in the wave-like (W) structures are usually tilted with respect to the geomagnetic meridian depicted in Figure 1. These tilts range from essentially zero (on January 24) to ~35° (on January 27). Exposure times were 6 s.

The observing conditions summarized in Figure 2 indicate a somewhat typical spectrum of viewing encountered in the Caribbean. The category "mostly clear" describes periods of photometric-caliber viewing conditions interrupted by brief periods of cumulus cloud passage. Virtually all of the data presented in this paper come from such conditions. Wave-like structures during "mostly cloudy" conditions refer to 6300-Å airglow structure seen at times of frequent cumulus cloud passage or through thin cirrus clouds spanning the FOV; photometric information is not reliable under such conditions, but morphology patterns can be recognized.

Plate 1 gives examples of 6300-Å wave-like (W) structures seen on the nights of January 24, 25, 26 and 27, 1993. As seen from the entries in Figure 2, W events tend to occur in the postsunset to postmidnight hours (0000-6000 UT corresponds to 2000-0200 lt at Arecibo). While additional data sets will justify use of the word wave to describe such structures, Plate 1 shows that the alternating bands of 6300-Å enhancements and depletions tend to be aligned in the northwest-southeast direction, with some variability from night to night. In most cases, however, they are not in the geomagnetic meridian, as depicted in Figure 1. The brightness level variations are typically ± 50 R from the image mean, except for the last example when much smaller variations were seen.

The night of January 27, 1993, was one treated in great detail, both observational and theoretically, by *Miller et al.* [this issue] due to the availability of Arecibo incoherent scatter and HF radar data throughout the night; it will not be discussed further here. To describe the overall characteristics of 6300-Å gravity wave effects, we will concentrate on January 25, 1993, the night with the longest sequence of W structure during the campaign, and one with supporting ionosonde data needed to understand the origin of 6300-Å variations produced primarily below the height of peak electron density in the F region (h_{max}).

Plate 2 gives a 2-hour sequence of images to show how the 6300-Å patterns typically evolve. The bands of emission and depletion are separated by ≤ 500 km (λ) and move slowly ($v \leq 100\ ms^{-1}$ toward the southwest throughout the night. This yields a period (P) at zenith of ~ 90 minutes, as shown in Plate 2 from 0139 to 0303 UT. Such parameters are typical of gravity waves

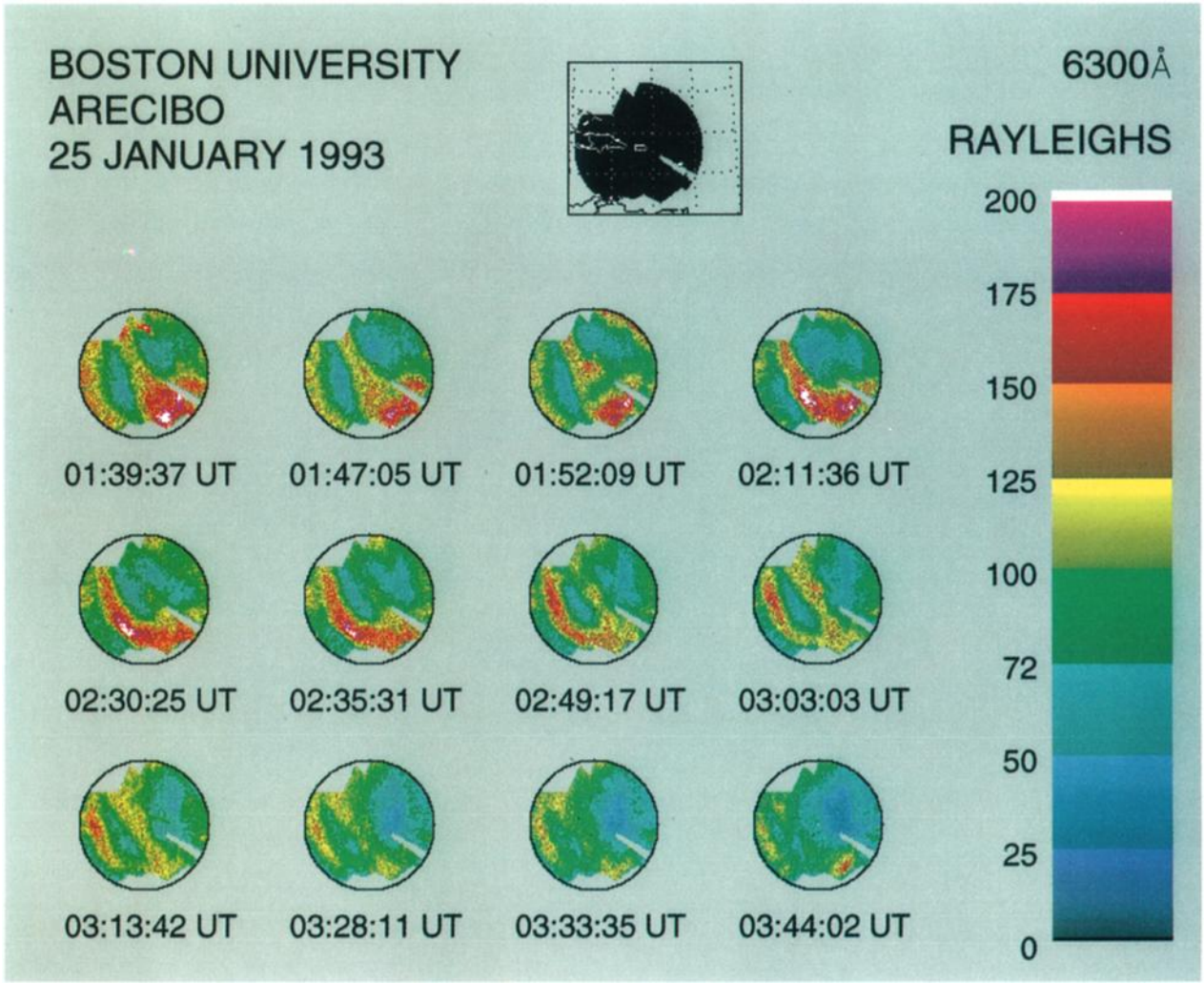

Plate 2. A sequence of images spanning a 2-hour period that exhibit the motion of gravity wave (W) structures through the field of view. These structures move from northeast to southwest at approximately 100 ms^{-1}.

seen as TIDs in the *F* region [*Hines*, 1960; *Yeh and Liu*, 1974; *Francis*, 1974]. At Arecibo they have been detected using the incoherent scatter radar [*Harper*, 1972], and by a scanning photometer [*Herrero and Meriwether*, 1981].

A possible source of 6300-Å structures in the *F* region, distinct from gravity wave origin, is one related to equatorial spread *F* (ESF). *F* region 6300-Å airglow depletions, aligned along or slightly tilted from a geomagnetic meridian, were first shown to be optical manifestations of ESF low electron content flux tubes spanning the geomagnetic equator by *Weber et al.* [1978]. Given that ESF associated airglow depletions can extend to great distances in altitude and latitude, occur preferentially in the postsunset hours, and appear in repetitive patterns [*Mendillo and Baumgardner*, 1982], the possibility exists that the features depicted in Plate 1 could be extraordinary cases of ESF patterns reaching to lower midlatitudes. *Sahai et al.* [1994] have shown that this is possible during periods of ESF, at any time in a solar cycle, from a site in the southern hemisphere (Cachoeira Paulista ≈16°S dip latitude) where observations at low elevation angles toward the south (elevation = 0°-15°) correspond to dip latitudes (25°-35°S) comparable to Arecibo's (≈ 29°N dip latitude) at zenith.

Several aspects of the features shown in Plates 1 and 2 suggest that they are not related to ESF airglow depletions. Perhaps foremost is the fact that equatorial airglow depletions drift with ambient plasma, typically to the east during the postsunset period; the features reported on here drift to the west. The visual characteristics of the features in Plates 1 and 2 are also very different from equatorial airglow depletions. Specifically, ESF effects produce bands of depleted airglow upon a uniform bright background; the Arecibo images suggest enhancements above a weak background airglow, or both enhancements and decreases with respect to ambient airglow. Said somewhat more qualitatively, to experienced observers of equatorial airglow depletions, the features in the Arecibo images do not look like equatorial airglow depletions. Finally, the nearby Digisonde at the Ramey Solar Observatory and the Cornell University HF radar (CUPRI) found little or no spread *F* on the night of January 25, 1993, or indeed for any of the nights shown in Plate 1 [*Miller*, 1996].

4. Modeling Gravity Wave Signatures in 6300-Å Airglow

The Digisonde [*Reinisch*, 1986; *Buchau et al.*, 1995], developed by the University of Massachusetts Lowell and

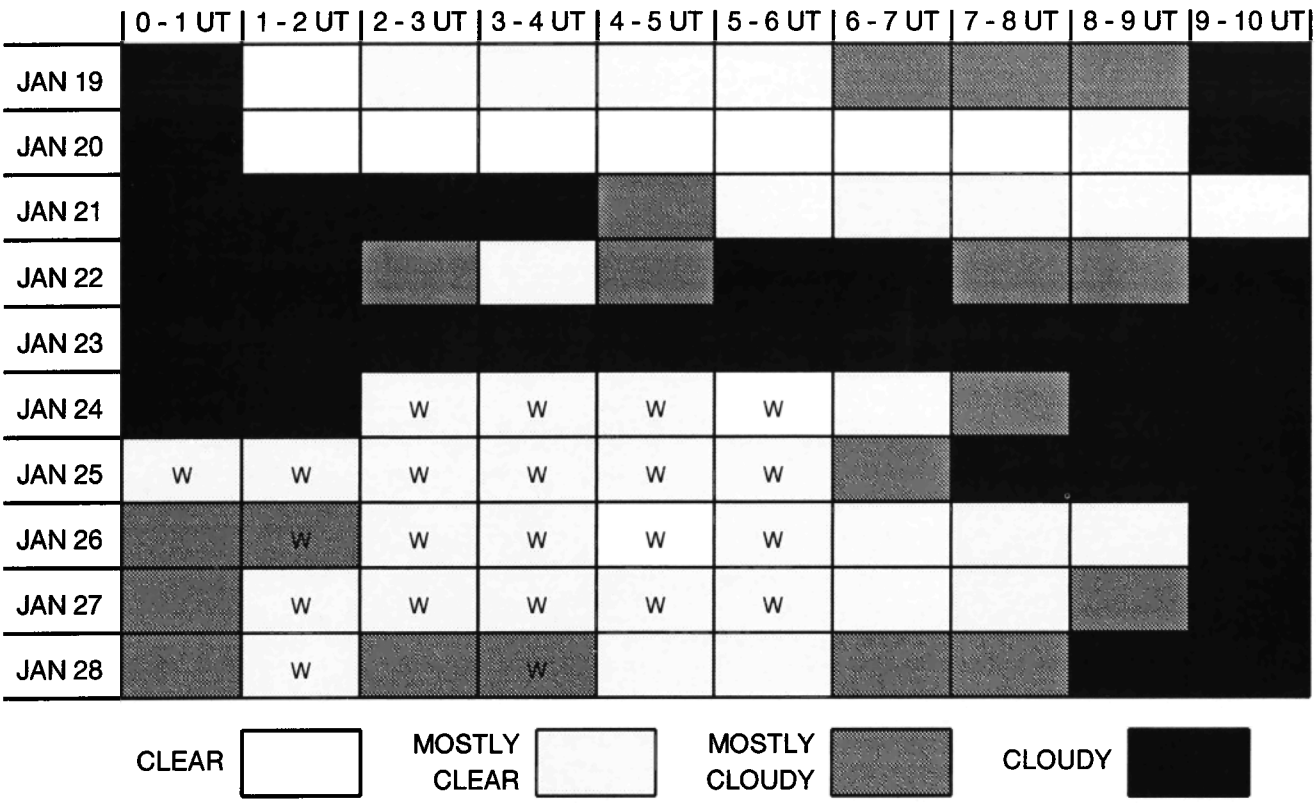

Figure 2. Summary of viewing conditions during the Mafongo Campaign in Arecibo, Puerto Rico, January 19-28, 1993. Conditions labeled "mostly clear" refer to clouds somewhere in the all-sky field of view. When confined to the horizon or to a rapid transit through the center of the FOV, such clouds do not prevent photometric calibration of the images somewhere during that hour. This is less true for "mostly cloudy" conditions. Hours marked with "W" refer to periods of wave- like structures in 6300 Å within the FOV.

operated by the U.S. Air Force at Ramey, Puerto Rico, is an ideal diagnostic instrument to monitor *F* region structure and dynamics for altitudes $\leq h_{max}$ [*Reinisch and Huang*, 1996]. Studies conducted by *Chen et al.* [1994] and *Scali et al.* [this issue] have shown how reliable estimates of the full electron density profile, $N_e(h)$, can be obtained on nights when Arecibo is not operating, or when it does so for only a limited time (as on January 25, 1993). Thus, for the entire night of optical observations (0000-8000 UT) true-height $N_e(h)$ profile are available (Figure 3a). One can see from Figure 3a that variations in h_{max} occurred, with TID-like vertical motions that are substantial. To test if these downward and upward motions of the *F* region into and away from the molecular oxygen [O_2] rich lower thermosphere are sufficient to produce the 6300-Å airglow variations observed, we conducted a modeling study using the $N_e(h)$ profiles from Figure 3a and the appropriate mass spectrometer incoherent scatter (MSIS) neutral atmosphere parameters for that night. Briefly, O (^1D) 6300-Å airglow is produced via the O_2 chain of *F* region loss:

$$O^+ + O_2 \rightarrow O_2^+ + O \quad (1)$$

$$O_2^+ + e^- \rightarrow O + O + \text{photons} \quad (2)$$

The volume emission rate ϵ_h in photons cm^3/s thus depends on the in situ O^+ and e^- (provided by the ionosonde), thermospheric species (provided by MSIS) that govern production of airglow (O_2) and O (^1D) quenching due to N_2, O_2, and O, plus the required reaction rates, quenching rates, Einstein coefficients, and branching ratios. A recent compilation of 6300-Å airglow parameters appears in the work of *Semeter et al.* [1996].

The integral with height of ϵ_h gives the total vertical column emission rate in Rayleighs (R),

$$E_{tot}(\text{R}) = 10^{-6} \int \epsilon_h(h)\, dh \quad (3)$$

Figures 3b gives the resultant ϵ_h versus height and time for the night of January 25, 1993, and Figure 4 gives a comparison between the modeled total emission (E_{tot}) and the observed zenith brightness levels extracted from the full set of images.

There are several noteworthy features in Figure 3. First, the variations in h_{max} (denoted by the thick line) exceed the [O_2] scale height (the MSIS parameters for this night give $T_\infty \approx$ 1000°K and thus $H = kT/mg$ for O_2 of ~30 km). This results in sufficient variations in the *F* region loss chemistry to produced observable variations in 6300-Å emission. As shown in Figure 3b, the height of peak emission $h_{max}(\epsilon)$ tracks h_mF2 in Figure 3a with offsets of 40 to 80 km. This questions the common practices of assuming that the airglow layer is about one scale height below h_{max}, or that it has a single height on a given night. Indeed, the use of a fixed height to portray images, as done in Figure 1 and Plates 1 and 2, is open to question in cases of detailed comparisons of positions of 6300-Å features. While

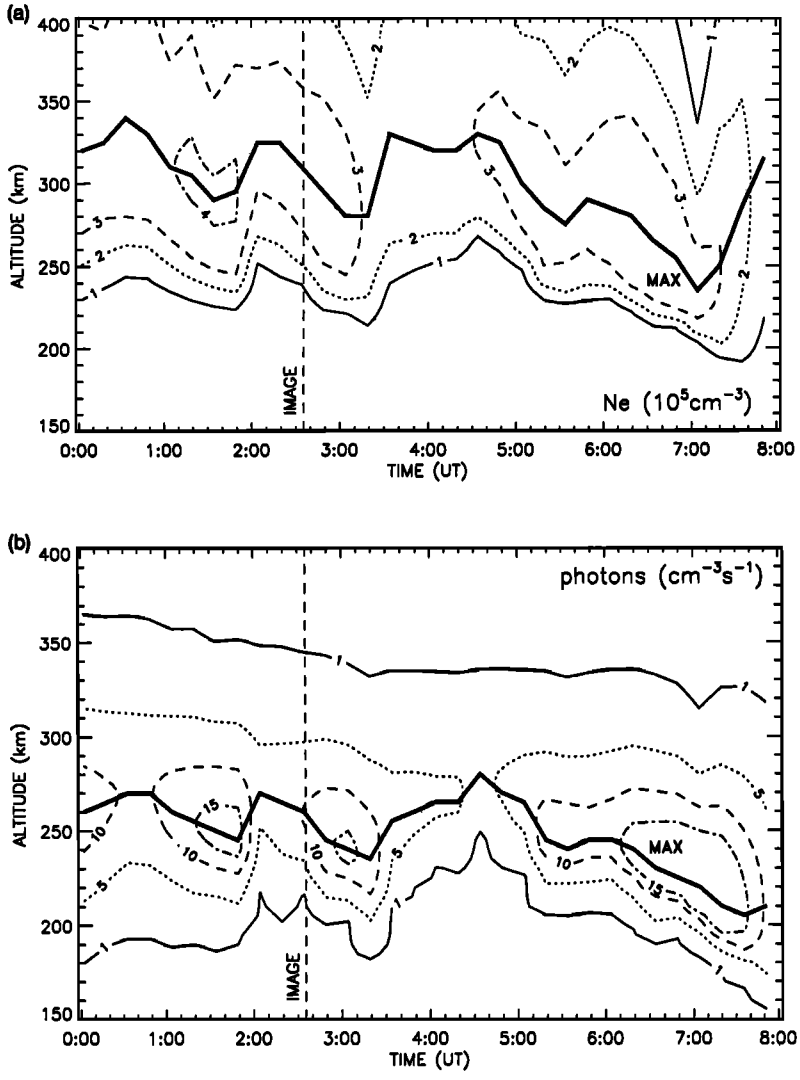

Figure 3. (a) Contours of electron density (N_e in 10^5cm^{-3}) on a vertical height versus time grid obtained from ionosonde data at Ramey Air Force Base in Puerto Rico on January 23, 1993, with topside extrapolations made using occasional $N_e(h)$ profiles obtained by the Arecibo incoherent scatter radar. Gravity wave patterns in electron density are shown best at $h \leq h_{max}$. These data are used to compute (b) the 6300 Å volume emission rate (photon cm^{-3}s^{-1}) airglow levels shown, as described in the text. The vertical dashed line in Figures 3a and 3b marks the time of the image at 0235:31 UT shown in Plate 1.

this is not the primary intent of this paper, modeling studies currently underway are looking into such geometrical factors that may contribute to the curvature of the wavefronts apparent in some of the images presented here.

The volume emission rate contours in Figure 3b also show that the 6300-Å airglow layer is really not a thin layer. The contour for 5 photons cm^{3}s^{-1}, essentially one third the peak emission, can span an altitude range of ~100 km. Above h_{max} ($\in$), there is little evidence of undulation activity in comparison to contours below h_{max} ($\in$), again suggestive of wave activity extending upward from the lower thermosphere. Finally, the excellent agreement in absolute values of observations and model results in Figure 4 is somewhat surprising given calibration uncertainties (±15-20%) and a host of reaction rate and MSIS uncertainties. Yet, similar levels of agreement were obtained for the other three nights shown in Plate 1, and thus we attach a high level of confidence to abilities to model gravity wave signatures in 6300-Å emission, at least under the conditions encountered in January 1993.

Link and Cogger [1988, 1989] reexamined the 6300-Å model-data comparisons conducted by *Cogger et al.* [1980] at Arecibo and reduced a factor of 2 discrepancy to ~ 10% using improved photochemical parameters. The *Semeter et al.* [1996] values used in our study are only slightly different from the Link and Cogger values, and thus we attached no particular significance to the approximately 20% discrepancy at peak brightness times in Figure 4. This discrepancy essentially vanishes at minimum brightness times, implying that a constant level of contamination from OH emission in the filter bandpass is probably not a concern; increased scattered light cannot be ruled out as a contamination issue during periods of bright emission near zenith. This might also be related to the "red line hysteresis" effect noted by *Cogger et al.* [1980], that is, measured brightness levels are generally higher than

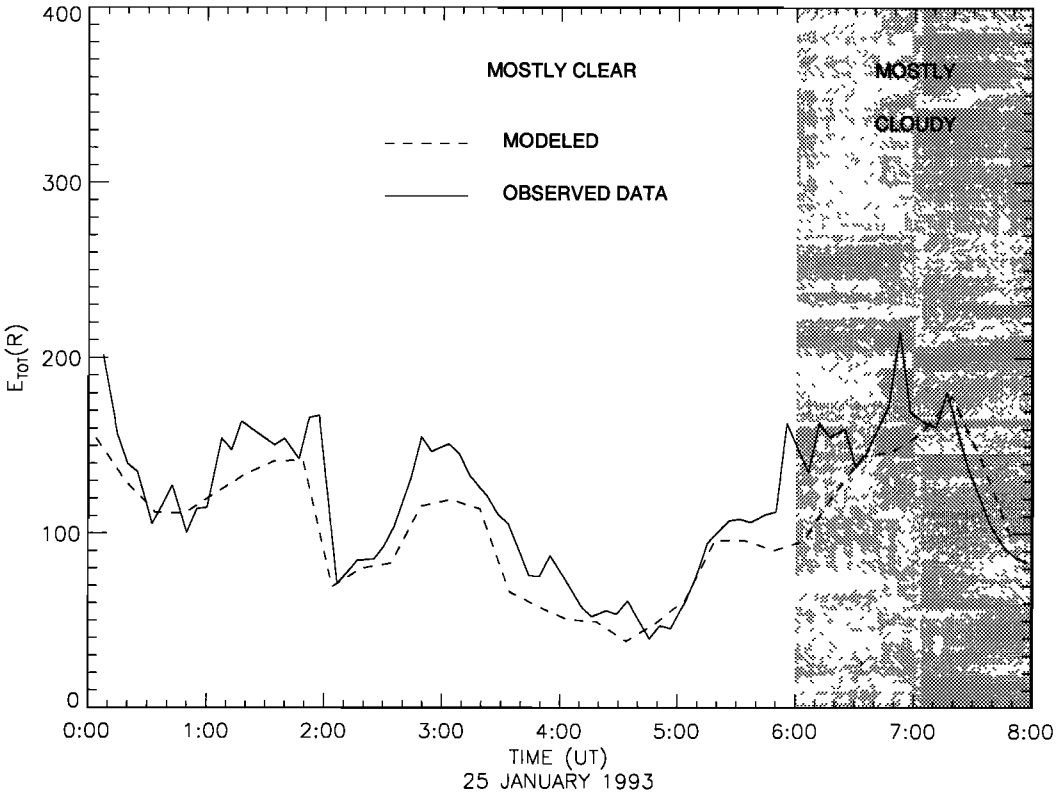

Figure 4. Comparison of observed 6300-Å brightness levels with computed total columnar brightness in Rayleighs obtained by vertical integration of the volume emission rates in Figure 3(b), using equation (3) in the text. Viewing conditions are given to illustrate how occasional clouds interfere with photometric calibration, as between 0600 and 0640 UT and at 0650 UT.

photochemical model predictions when the brightness is decreasing due to a rising *F* region.

5. Thermospheric Dynamics: Wind Induced Airglow Enhancements

A persistent feature of the low latitude thermosphere is the so-called midnight temperature maximum (MTM), a region of anomalous temperature and density that is generally considered to result from atmospheric tidal interactions [*Mayr et al.*, 1979; *Herrero et al.*, 1993; *Fesen*, 1996]. This pressure bulge has a seasonal-latitudinal pattern of occurrence that can extend beyond ± 20° geographic latitudes [*Herrero and Spencer*, 1982] (see also *Herrero et al.* [1993] for a review). Winds generated from the MTM pressure bulge propagate northward and at Arecibo's latitude (dip angle ≈ 50°) move *F* region plasma downward to regions of enhanced loss and airglow production. This phenomenon at Arecibo has been called the "midnight descent" [*Nelson and Cogger*, 1971], "midnight collapse" [*Sobral et al.*, 1978], and the "meridional intensity gradient (MIG)" by *Herrero and Meriwether* [1980, 1994]. During the 1993 observing campaign, this effect was not observed (see Figures 3 and 4), but it did appear in our subsequent 1995 campaign.

Recent imaging observations conducted in Arequipa, Peru, have shown that the MTM-induced winds produce a brightness wave in 6300-Å emission that propagates across the all-sky field of view [*Colerico et al.*, 1996; M. Mendillo et al., 1997]. The seasonal occurrence pattern of the brightness wave showed maxima in October and minimum in solstice months. A preliminary search of our second observing campaign in Arecibo (February to August 1995) revealed cases of brightness wave events on April 24 and 27 and July 1 and 2. An example is given in Figure 5. As described in by Mendillo et al. [1997], a full night's worth of images can be sampled along the north-south meridian to create a latitude versus time history for 6300-Å. This is essentially the same as obtained from a scanning photometer system except that each scan is extracted from a single image and therefore at the same time. The pattern in Figure 5 is one of a brightness wave that moves northward with a S-N phase speed of ~ 300 ± 30 ms^{-1} during the post midnight hours (0500-0600 UT). This is consistent with the first detection of such transient features in 6300-Å brightness (i.e., *Sobral et al.*, [1978] also reported meridinal phase speeds of ~ 300 ms^{-1}).

As described by *Colerico et al.* [1996], an MTM pattern fixed in local time, encountered by an imaging system at its corotational speed (V_{co}), results in a meridional phase speed (V_{s-n}) dependent on the tilt (θ) of the feature with respect to the meridian. Algebraically,

$$\tan \theta = V_{co}/V_{s-n} \quad (4)$$

which, for the case of Arecibo (where V_{co} = 440 ms^{-1}), results in $\theta \approx 55°$ for V_{s-n} = 300 ms^{-1}. Such tilt angles are typical of midnight pressure bulge morphology patterns described using satellite observations [*Herrero and Spencer*, 1982] and optically

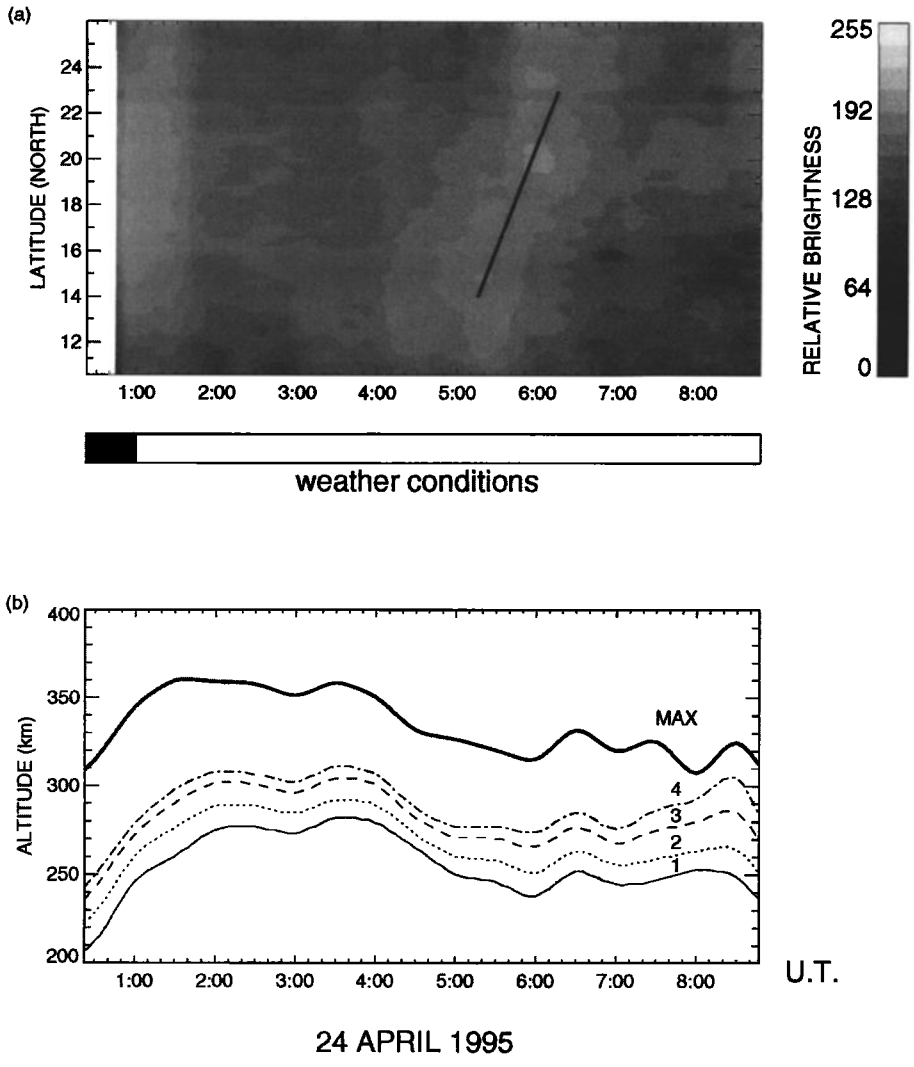

Figure 5. (a) Example of 6300-Å brightness wave morphology using north- south scans of images versus time on April 24, 1995, at Arecibo, Puerto Rico. The 6300-Å brightness values are assigned latitudes using an airglow emission height 300 km. The slope of the line of maximum brightness gives an effective north-south wave speed component of 301 ± 29 ms^{-1}. In order to avoid using brightness signatures at the edges of the field of view, the linear fit to the peak brightness pattern was done between zenith angles of ± 60°, corresponding to latitudes 14° to 23°N. (b) Contours of $N_e(h)$ in units of $10^5 cm^{-3}$ versus time obtained from ionosonde observations at Ramey, Puerto Rico, on the night of April 24, 1995.

by *Colerico et al.* [1996]. Thus, brightness wave effects caused by meridional winds that flow from the MTM pressure bulge can be used to specify the two-dimensional characteristics of midnight collapse patterns at midlatitudes. In addition, they provide a potentially useful diagnostic of the night-to-night variations of the MTM pattern itself and thereby its origin via tidal mode interactions. Current models (empirical and theoretical) have yet to achieve full success in specifying MTM amplitudes [*Colerico et al.*, 1996], though considerable progress has been made recently [*Fesen*, 1996].

Digisonde profiles taken on the night of the brightness wave event are presented in Figure 5b. The classic signature of a lowering of h_{max} to regions of enhanced loss (and therefore 6300-Å production) is clearly evident from 0400-0600 UT. The magnitude of the poleward winds, U, that drive the F layer downward may be estimated using the descent of the 10^5 electrons cm^3 contour in Figure 5b. The resultant vertical motion of 30 km from 0400 to 0500 UT corresponds to a plasma drift of ~ 8.3 ms^{-1}; equating this to $U \sin I \cos I$ yields U ~ 17 ms^{-1} as an estimate of meridianal wind driven by the midnight pressure bulge. It should be noted that this is a separate effect from the ~300 ms^{-1} phase speed at which the MTM induced feature passes through the image's FOV. Finally, $U \approx 17$ ms^{-1} is also the wind estimated in the absence of electric fields. An eastward E, generated by the F layer dynamo, would tend to support the layer, and thus a somewhat larger neutral wind would be required to produce the airglow signatures observed.

The topic of sources for MTM-induced dynamics, a somewhat dormant subject for the last decade or so, has been invigorated recently by new model studies [e.g., *Fesen*, 1996], observations [e.g., *Colerico et al.*, 1996], and new analysis of past data [e.g., *Herrero and Meriwether*, 1994]. *Goembel and Herrero* [1995] have also suggested from a new analysis of Atmospheric Explorer satellite data that intensifications of winds from the nighttime pressure bulge are better correlated with solar activity indicators (specifically the F10.7 index) than

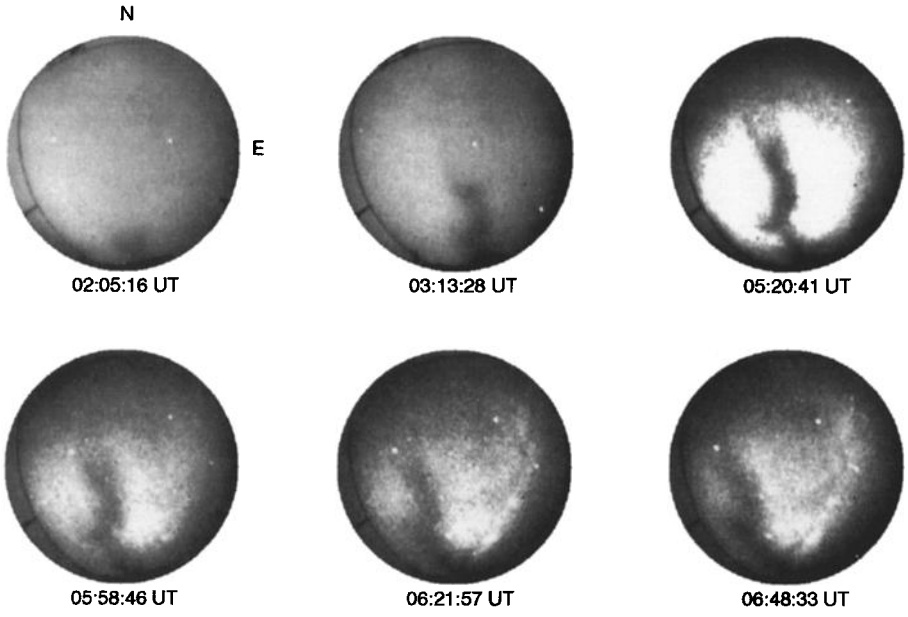

Figure 6. A sequence of all-sky images in 6300-Å on May 3, 1995, at Arecibo, Puerto Rico, that portrays the evolution of an airglow depletion associated with equatorial spread *F* (ESF) patterns. The extension of the depletion northward of Arecibo's zenith at 0520:41 UT describes the occurrence of a plasma depleted flux tube that maps to altitudes above the L=1.4 (h≈2500 km) domain at the geomagnetic equator.

with geomagnetic activity indices. They argue that variations in solar EUV input on the dayside hemisphere are more important than auroral sources for causing nighttime wind abatements. The interplay between solar-driven tides and traveling atmospheric disturbances (TADs) from the auroral zones certainly warrants further study, both via modeling and observations beyond our limited data set, to explore the "EUV vs. Kp" scenarios suggested by Goembel and Herrero (1995).

6. Equatorial Spread *F* (ESF) Effects

As mentioned in sections 2 and 3, one would not expect equatorial plasma instabilities ("ESF") and their 6300-Å optical signature ("airglow depletions") to extend to Arecibo's location at ~ 30° dip latitude (L = 1.4) on a regular basis. Routine airglow observations are made at low latitudes in the American sector at only two sites: Arequipa (Peru) at 16.4°S, dip latitude ≈4°S (Mendillo et al., 1997) and Cachioera Paulista (Brazil) at 23°S, dip latitude ≈ 16°S [*Sahai et al.*, 1994]. The Arequipa site is relatively close to the geomagnetic equator, and thus airglow depletions at the southern edge of its imaging system's field of view (FOV) pertain to plasma depleted flux tubes ("ESF bubbles") that have apex heights of ~ 1000 km above the geomagnetic equator.

In Brazil the Cachioera Paulista FOV extends to much greater distances away from the magnetic equator, and thus airglow depletions can map to apex heights of $h \geq 1500$ ($L \geq 1.25$). *Sahai et al.* [1994] have given several examples of such high-altitude, high-latitude plumes. Arecibo's location is still further away from the geomagnetic equator, and thus airglow depletions reaching its zenith would be associated with L = 1.4 flux tubes, or apex heights of $h \geq 2500$ km. An example of such a high-altitude ESF plume, as inferred from 6300-Å airglow depletions, is given in Figure 6. Note that the depletion moves from south to north (i.e., to higher L values) and drifts to the east, both classic signatures of ESF evolution in the postsunset time period. The eastward drift is slow, and after midnight (0400UT) the airglow depletion is almost stationary or moves slowly westward.

The month of May is not one of routine occurrence of airglow depletions in the American longitude sector [*Aarons*, 1993; *Sahai et al.*, 1994; Mendillo et al., 1997]. Events during "non-

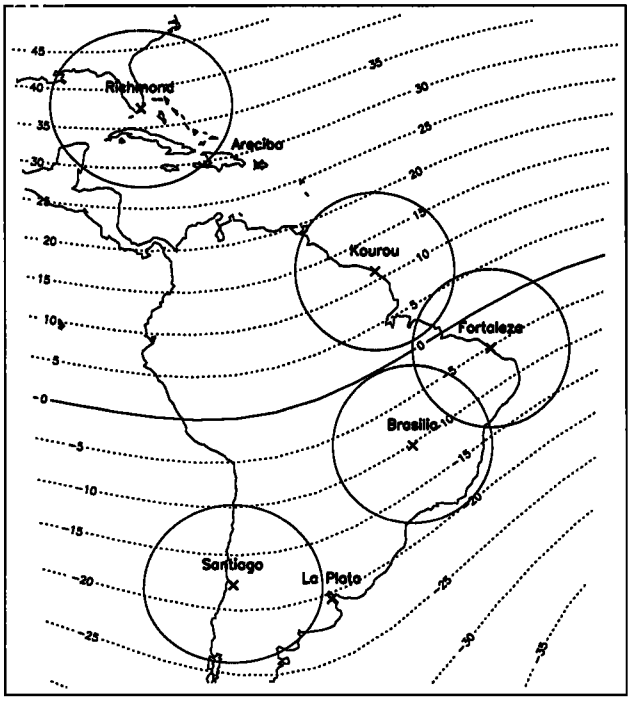

Figure 7. Locations of Global Positioning System (GPS) satellite observing sites operational in the Arecibo longitude sector on the night of May 3, 1995. At each site, satellites are observed over a ±75° zenith angle field of view, as indicated by the circular regions. Total electron content (TEC) data from these stations are given in Figure 8.

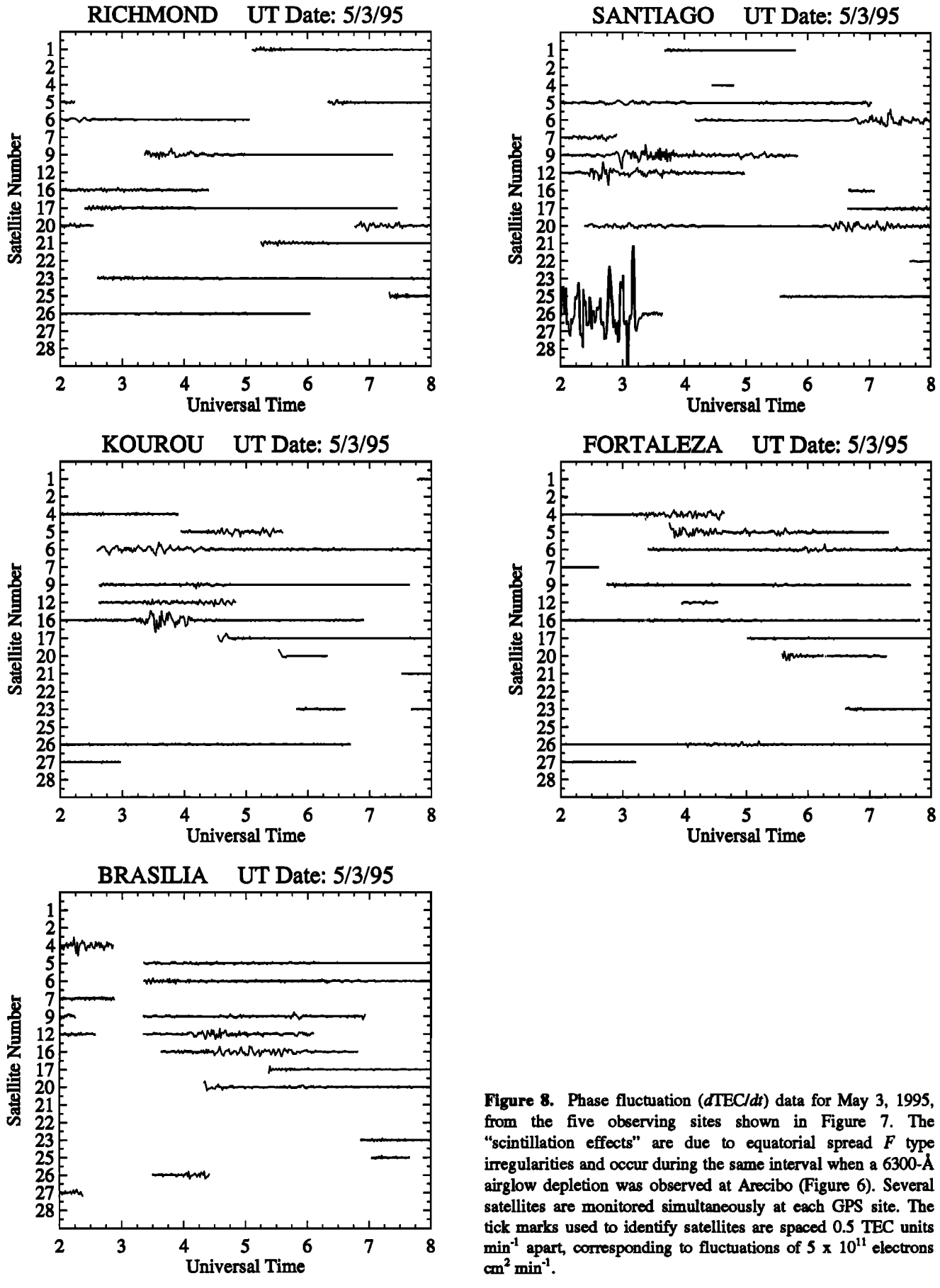

Figure 8. Phase fluctuation (dTEC/dt) data for May 3, 1995, from the five observing sites shown in Figure 7. The "scintillation effects" are due to equatorial spread F type irregularities and occur during the same interval when a 6300-Å airglow depletion was observed at Arecibo (Figure 6). Several satellites are monitored simultaneously at each GPS site. The tick marks used to identify satellites are spaced 0.5 TEC units min^{-1} apart, corresponding to fluctuations of 5 x 10^{11} electrons cm^2 min^{-1}.

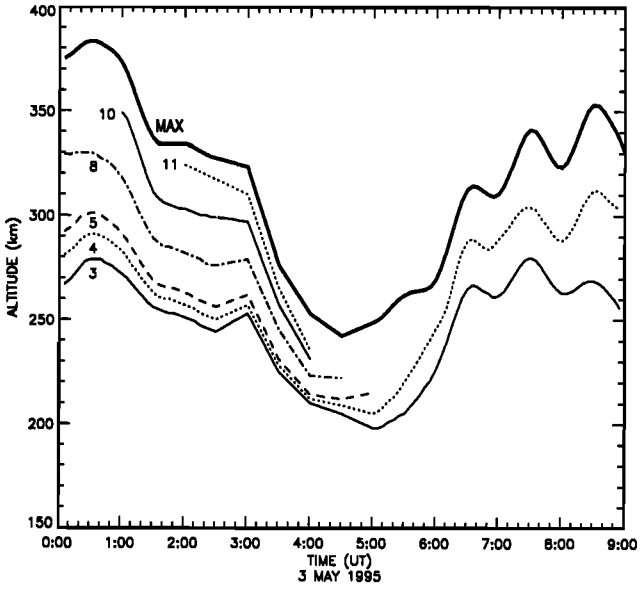

Figure 9. Contours of $N_e(h)$ in units of $10^5 cm^{-3}$ versus time obtained from ionosonde observations at Ramey, Puerto Rico, on the night of May 3, 1995. The very large decrease in F layer height was associated with f_0F2 values increasing to ~ 13 MHz.

ESF-season" can occur, however, often in conjunction with geomagnetic activity [*Aarons*, 1991]. To confirm that ESF activity was indeed present on this night, we examined all available Global Positioning System (GPS) data from the Caribbean - South American region. *Aarons et al.* [1996] have shown that 30-s GPS observations of total electron content (TEC) can be used to calculate phase fluctuations (dTEC/dt), and that these have a correlation with the radio amplitude scintillations and 6300-Å airglow depletions usually associated with ESF onset and growth. Figure 7 gives a map of the distribution of GPS sites operational on the night of May 3, 1995. To the west of Arecibo's longitudes, data are available from a more northward site (Richmond, Florida), as well as from the equatorial anomaly site in Santiago (Chile). To the east of Arecibo, GPS sites in Brazil include one near the geomagnetic equator (Fortaleza) and one near the southern anomaly region (Brasilia). In the northern anomaly region, data were available from Kourou (French Guiana). All of these data sets are displayed in Figure 8. While phase fluctuations (as described by dTEC/dt) were not severe, they were clearly of the type described by *Aarons et al.* [1996] for irregularities associated with ESF patterns during geomagnetic storms. Indeed, May 3, 1995 was a somewhat disturbed day with $Dst \approx -50$ nT and Kp = 5-6 for the 0000-9000 UT period.

We conclude from the observations in Figures 6 and 8 that an unusually high-altitude, high-latitude equatorial plasma depletion and irregularity pattern occurred on May 3,1995, with Rayleigh-Taylor instability effects extending to $L \geq 1.4$. There were no images in Figure 6 from 0313 to 0520 UT due to unusually bright 6300-Å emission which saturated the all-sky detector system. When observations were again possible after 0500 UT (0100LT), the 6300-Å airglow was still very bright, suggesting pronounced midnight-collapse effects, as discussed earlier. Local ionosonde observations from Ramey are given in Figure 9. From 0300 to 0430 UT, $h_{max}F2$ decreased by nearly 90 km, and peak density values increases to over 10^6 electrons cm^3. Spread F conditions occurred in the ionogram traces for the rest of the night, but not of such severity as to prevent use of the data to extract the $N_e(h)$ patterns shown.

7. Conclusion

Two periods of pilot observations using an all-sky imaging system at 6300-Å to record large-scale F layer irregularity patterns have been conducted at the Arecibo Observatory in 1993 and 1995. Prior photometer studies of 6300-Å events at Arecibo conducted by *Herrero and Meriwether* [1981] had suggested that the Arecibo region was susceptible to a host of tropical latitude coupling process. Yet, wide-angle, low-light-level imaging investigations of F region red line structures were never attempted in a systematic fashion. Thus the results obtained here represent the first two-dimensional observations of red line gravity wave signatures in the thermosphere-ionosphere system, of midnight pressure bulge generated wind signatures upon 6300-Å airglow, and of equatorial plasma instability processes upon airglow at lower midlatitudes. Coordinated observations using the Digisonde at Ramey (PR) during each of these phenomena have been used to model gravity wave signatures in 6300-Å and to assist in the interpretations of MTM and ESF effects. The Global Positioning System (GPS) satellite monitoring network in the Caribbean and South American sector was also used to relate plasma irregularities spanning the equatorial region to 6300-Å airglow depletion effects at Arecibo. Each of these pilot studies introduced a view of thermospheric-ionospheric coupling and dynamics not easily obtained using single diagnostic systems. Additional imaging science observations and modeling will be able to address these topics in a more comprehensive way in the years ahead, as well as provide context for active experiments that induce or are affected by ambient structures at Arecibo [*Bernhardt et al.*, 1989, *Rowland and Bernhardt*, 1991].

Acknowledgements. At Boston University this work was supported in part by NSF grant ATM 92-01398. P. Sultan, X. Q. Pi, J. Noto, J. Semeter, and M. Colerico assisted in various aspects of equipment setup and observations, and M. Colerico assisted in analysis of the images. The GPS data used in this study were provided by NASA/JPL as part of the International GPS Service (IGS) for Geodynamics, and R. Yantosca assisted in their analysis with support from ONR and NASA. The University of Massachusetts Lowell effort was supported by AF contract F19628-90-K-0029 and by NSF grant ATM-9415707. Z. Kecic of UML assisted in the preparation of the profile data. We are indebted to the U.S. Air Force Air Weather Service and the staff at Ramey Solar Observatory for their support of the research campaigns. At Cornell University this work was supported by NSF grant ATM-9415815, and C. Miller assisted with the data analysis. At the Arecibo Observatory the director and staff offered collegial assistance and cooperation throughout the 1993 and 1995 observations. We are particularly indebted to Craig Tepley for organizing and coordination of our visits and to Paul Castleberg (Cornell University) and Jonathan Friedman of the Observatory for their cooperation.

The Editor thanks J. W. Meriwether and P. A. Bernhardt for their assistance in evaluating this paper.

REFERENCES

Aarons, J., The role of the ring current in the generation or inhibition of equatorial F layer irregularities during geomagnetic storms, *Radio Sci.*, *26*, 1131, 1991.

Aarons, J., The longitude morphology of equatorial F-layer irregularities relevant to their occurrences, *Space Sci. Rev.*, *63*, 209, 1993

Aarons, J. , M. Mendillo, R. Yantosca, and E. Kudeki, GPS phase fluctuations in the equatorial region, *J Geophys. Res.*, in press, 1996.

Baumgardner, J., B. Flynn, and M. Mendillo, Monochromatic imaging instrumentation for applications in aeronomy of the Earth and planets, *Opt. Eng.*, *32*, 3028, 1993.

Bernhardt, P.A., L.M. Duncan, and C.A. Tepley, Artificial airglow executed by high-power radio waves, *Science, 242, 1022*, 1988a.

Bernhardt, P.A., B.A. Kashiwa, C.A. Tepley, and S.T. Noble, Spacelab-2 Upper Atmospheric Modification Experiment over Arecibo, 1, Neutral gas dynamics, *Astrophys. Lett. Commun.*, *7*, 169, 1988b.

Bernhardt, P. A., et al., Airglow enhancements associated with plasma cavities formed during ionospheric heating experiments, *J. Geophys. Res.*, *94*, 9071, 1989.

Buonsanto, M. J., J. C. Foster, and D. P. Sipler, Observations from Millstone Hill during the geomagnetic disturbances of March and April 1990, *J. Geophys. Res.*, *97*, 1225, 1992.

Buchau J., T. W. Bullett, A. E. Ronn, K. D. Scro, and J. L. Carson, The digital ionospheric sounding system network of the US Air Force Weather Service, *Rep. UAG-104*, p. 16 World Data Cent. A for Sol.-Terr. Phys., Colo., 1995.

Burnside, R. G., F. A. Herrero, J. W. Meriwether, and J. C. G. Walker, Optical observations of thermospheric dynamics at Arecibo, *J. Geophys. Res.*, *86*, 5532, 1981.

Campbell, D., Upgrade Project, National Astronomy and Ionosphere Center, *Newsl.* 17, Arecibo Obs., Arecibo, Puertor, Oct. 1995.

Carlson, H. C., Most recent studies of low latitude effects due to conjugate location heating, *Radio Sci.*, *3*, 668, 1968.

Chen, C. F. , B. W. Reinisch, J. L. Scali, X. Huang, R. R. Gamache, M. J. Buonsanto, and B. D. Ward, The accuracy of ionogram-derived N(h) profiles, *Adv. Space Res.*, *14*(12), 43-46, 1994.

Colerico, M., M. Mendillo, D. Nottingham, J. Baumgardner, J. Meriwether, J. Mirick, B. Reinisch, J. Scali, and C. Fessen, Coordinated measurements of *F* region dynamics related to the thermospheric midnight temperature maximum, *J. Geophys. Res.*, in press, 1996.

Cogger, L. L., G. J. Nelson, M. A. Biondi, R. D. Hake, and D. P. Sipler, Coincident *F* region temperature determined from incoherent backscatter and Doppler broadening of [OI] 6300-Å, *J. Geophys. Res.*, *75*, 4887, 1970.

Cogger, L. L., J. C. G. Walker, J. W. Meriwether Jr., and R. G. Burnside, *F* region airglow: Are groundbased observations consistent with recent satellite results?, *J. Geophys. Res.*, *85*, 3013, 1980.

Fesen, C. G., Simulations of the low latitude midnight temperature maximum, *J. Geophys. Res.*, in press, 1996.

Foster, J. C., M. J. Buanonsanto, M. Mendillo, D. Nottingham, F. J. Rich, and W. Denig, Coordinated stable auroral red arc observartions: Relationship to plasma convection, *J. Geophys. Res.*, *99*, 11429, 1994.

Francis, S. H., A theory of medium-scale traveling ionosphere disturbances, *J. Geophys. Res.*, *79*, 5245, 1974.

Friedman J. S., P. A. Castleberg, K. A. Dighe, C. A. Tepley, and M. C. Kelley, The Arecibo Observatory lidar upgrade: Possibilities for new science, *Opt. Remote Sens. Atmos. Tech. Dig.*, *5*, 189-192, 1993.

Fukao, S., M. C. Kelley, T. Takami, M. Yamamato, T. Tsuda, and S. Kato, Turbulent upwelling of the mid-latitude ionosphere, 1, Observational results by the MU radar, *J. Geophys. Res.*, *96*, 3725, 1991.

Gordon, W. E., Arecibo Ionospheric Observatory, *Science*, *146*, 26, 1964.

Goembel, L., and F. A. Herrero, Anomalous meridional thermospheric neutral winds in the AE-E NATE data: Effects of the equatorial nighttime pressure bulge, *Geophys. Res. Lett.*, *22*, 271, 1995.

Hanson, W. B., and R. J. Moffett, Ionozation transport effects in the equatorial *F* region, *J. Geophys. Res.*, *71*, 5559, 1996.

Harper, R. M., Observations of a large nighttime gravity wave at Arecibo, *J. Geophys. Res.*, *77*, 1311, 1972.

Hecht, J. H., R. L. Walterscheid, and M. N. Ross, First measurements of the two-dimensional wave number spectrum from CCD images of nightglow, *J. Geophys. Res.*, *99*, 11449, 1994.

Herrero, F. A., and J. W. Meriwether, 6300-Å Airglow meridional intensity gradients, *J. Geophys. Res.*, *85*, 4191, 1980.

Herrero, F. A., and J. W. Meriwether, Equatorial night-time F-region events: A survey of 6300 Å airglow intensity maps at Arecibo, *J. Atmos. Terr. Phys.*, *43*, 859, 1981.

Herrero, F. A., and J. W. Meriwether, The 630nm MIG and the vertical neutral wind in the low latitude nighttime thermosphere, *Geophys. Res. Lett.*, *21*, 97, 1994.

Herrero, F. A., and N. W. Spencer, On the horizontal distribution of the equatorial thermospheric midnight temperature maximum and its seasonal variation, *Geopyhs. Res. Lett.*, *9*, 1179, 1982.

Herrero, F. A., N. W. Spencer, and H. G. Mayr, Thermosphere and *F* region plasma dynamics in the equatorial region, *Adv. Space. Res.*, *13*, 202, 1993.

Hines, C., Internal atmospheric gravity waves in the upper atmosphere, *Can. J. Phys.*, *38*, 1441, 1960.

Hines, C. O., Ionospheric movements and irregularities, in Research in Geophysics (edited by H. Odishaw, pp. 299-318, MIT Press, Cambridge, Mass., 1964.

Kane, T. J., C. S. Gardner, Q. Zhou, J. D. Matthews, and C. A. Tepley, Lidar, radar and airglow observations of a spectacular sporadic Na/sporadic *E* Layer event at Arecibo during AIDA-89, *J. Atmos. Terr. Phys.*, *55*, 499-511, 1993.

Kelley, M. C., The Earth's Ionosphere: Plasma Physics and Electrodynamics, Academic, San Diego, Calif., 1989.

Kelley, M. C., and S. Fukao, Turbulent upwelling of the mid-latitude ionosphere, 2, Theoretical framework, *J. Geophys. Res.*, *96*, 3747, 1991.

Kerr, R. B., and C. A. Tepley, Ground-based measurements of exospheric hydrogen densities, *Geophys. Res. Lett.*, *15*, 1329, 1988.

Link, R., and L. L. Cogger, A reexamination of the OI 6300-Å nightglow, *J. Geophys. Res.*, *93*, 9883, 1988.

Link, R., and L. L. Cogger, Correction to "A reexamination of the OI 6300-Å nightglow," *J. Geophys. Res.*, *94*, 1556, 1989.

Mayr, H. G., I. Harris, N. W. Spencer, A. E. Hedin, L. E. Wharton, H. S. Porter, J. C. G. Walker, and H. Carlson, Atmospheric tides and the midnight temperature anomaly in the thermosphere, *Geophys. Res. Lett.*, *6*, 447, 1979.

Mendillo, M. and J. Baumgardner, Airglow characteristics of equatorial plasma depletions, *J. Geophys. Res.*, *87*, 7641, 1982.

Mendillo, M., J. Baumgardner, J. Aarons, J. Foster, and J. Klobuchar, Coordinated optical and radio studies of ionospheric disturbances: Initial results from Millstone Hill, *Ann. Geophys.*, *5*(6), 543, 1987.

Mendillo, M., J. Baumgardner, M. Colerico, and D. Nottingham, Imaging science contributions to equatorial aeronomy: Initial results from the MISETA program, *J. Atmos. Terr. Phys.*, in press, 1996.

Mendillo, M., J. Semeter, and J. Noto, Finite Element Simulation (FES): A Computer modeling techniques for studies of chemical modification of the ionosphere, *Adv. Space Res.*, *13*,(10), 55, 1993.

Mendillo, M., J. Baumgardner, and J. Privodakes, Ground based imaging of detached arcs, ripples in the diffuse aurora, and patches of 6300-Å emission, *J. Geophy. Res.*, *94*, 5367, 1989.

Mendillo, M., Baumgardner, J., Pi, X.-Q., Sultan, P., Tsunoda, R., Onset conditions for equatorial spread, *J. Geophys. Res.*, *97*, 13865, 1992.

Meriwether, J. W., Jr., S. K. Atreya, T. M. Donahue, and R. G. Burnside, Measurements of the spectral profile of Balmer alpha emissons from the hydrogen geocorona, *Geophys. Res. Lett.*, *7*, 967, 1980.

Miller, C. A., On gravity Waves and the electrodynamics of the mid-latitude ionosphere, Ph.D. Dissertation, Cornell Univ., Jan., 1996.

Miller, C. A., W. E. Swartz, M. C. Kelley, M. Mendillo, D. Nottingham, J. Scali, and B. Reinisch, Electrodynamics of midlatitude spread *F*, 1, Observations of unstable, gravity wave-induced ionospheric electric fileds at tropical latitudes, *J. Geophys. Res.*, this issue, 1996.

Nelson, G. J., and L. L. Cogger, Dynamical Behavior of the Nighttime Ionosphere at Arecibo, *J. Atmos. Terr. Phys.*, *33*, 1711, 1971.

Providakes, J. F., M. C. Kelley, W. E. Swartz, M. Mendillo, and J. Holt, Radar and optical measurements of ionospheric processes associated with intense subauroral electric fields, *J. Geophys. Res.*, *94*, 5350, 1989.

Reinisch, B. W., New techniques in ground-based ionospheric sounding and studies, *Radio Sci.*, *21*, 331, 1986.

Reinisch, B. W., and X. Huang, Low latitude digisonde measurements and comparison with IRI, *Adv. Space Res.*, *18*, 6, 5-12, 1996.

Rishbeth, H. and O. K. Garriott, Introducton to Ionospheric Physics Academic, San Diego, Calif., 1969.

Roach, F. E., Variations of [IO] 5577Å emission in the upper atmosphere, *Ann. Geophys.*, *17*, 172, 1961.

Rowland, H. L., and P. A. Bernhardt, A nonlinear oscillator in the ionosphere: beam snapback during RF heating, in Physics of Space Plasmas, *SPIE Conf. Proc. Reprint Ser.*, pp. 335-348, Scientific, Cambridge, Mass. 1991.

Sahai, Y., J. Aarons, M. Mendillo, J. Baumgardner, J.A. Bittencourt, and H. Takahashi, OI 630 nm imaging observations of equatorial plasma depletions at 16°S dip latitude, *J. Atmos. Terr. Phys.*, *56*, 1461, 1994.

Scali, J., B. Reinisch, C. A. Miller, M. C. Kelley, W. E. Swartz, and Q. Zhou, Comparison of incoherent scatter radar and digisonde techniques

at tropical latitudes including conjugate point observations, *J. Geophys. Res.*, this issue.

Semeter, J., M. Mendillo, J. Baumgardner, J. Holt, D. E. Hunton, and V. Eccles, A study of oxygen 6300 Å airglow production through chemical modification of the nighttime ionosphere, *J. Geophys. Res.*, *101*, 19683, 1996.

Sobral, J. H. A., H. C. Carlson, D. T. Farley, and W. E. Swartz, Nighttime dynamics of the *F* region near arecibo as mapped by airglow features, *J. Geophys. Res.*, *83*, 2561, 1978.

Taylor, M., and F. J. Garcia, A two-dimensional spectral analysis of short period gravity waves imaged in the OI (557.7nm) and near infra red OH nightglow emissions over Arecibo, Puerto Rico, *Geophys. Res. Lett*, *22*, 2473, 1995.

Tepley, C., Atmospheric science highlights, *Newsl.* 17, Nat. Astron. and Ionos. Cent., Arecibo Obs., Arecibo, Puerto Rico, October 1995.

Tepley, C. A., S. I. Sarggoychev, and C. O. Hines, Initial Doppler Rayleigh lidar results from Arecibo, *Geophys. Res. Lett.*, *18*, 167-170, 1991.

Van Zandt, T. E., and V. L. Peterson, Detailed maps of tropical 6300Å nightglow enhancements and their implications on the F_2 layer, *Ann. Geophys.*, 24(3), 747, 1968.

Weber, E. J., J. Buchau, R. Eather, and S. B. Mende, North-south aligned equatorial airglow depletions, *J. Geophys. Res.*, *83*, 712, 1978.

Yeh, K. C., and C. H. Lin, Acoustic-gravity waves in the upper atmosphere, *Res. Geophys.*, *12*, 193, 1974.

J. Aarons, J. Baumgardner, M. Mendillo and D. Nottingham, Center for Space Physics, Boston University, 725 Commonwealth Avenue, Boston, MA 02215. (e-mail: mendillo@buasta.bu.edu)

M. Kelley, School of Electrical Engineering, Cornell University, 318 Engineering and Theory Center, Ithaca, NY 14853. (E-mail: mirek@magneto.ee.cornell.edu)

B. Reinisch and J. Scali, Center for Atmospheric Research, University of Massachusetts, 450 Aiken Street, Lowell, MA 01854. (E-mail: reinisch@cae.ulowell.edu; scali@woods,ulowell.edu)

(Received March 28, 1996; revised September 4, 1996;
accepted September 6, 1996.)